PHYSICAL REVIEW E **88**, 030701(R) (2013)

Localizing epileptic seizure onsets with Granger causality

Bhim M. Adhikari,[1] Charles M. Epstein,[2] and Mukesh Dhamala[3]
[1]*Department of Physics and Astronomy, Georgia State University, Atlanta, Georgia 30303-4106, USA*
[2]*Department of Neurology, Emory University School of Medicine, Atlanta, Georgia 30322, USA*
[3]*Department of Physics and Astronomy, Neuroscience Institute, Center for Behavioral Neuroscience, Georgia State and Georgia Tech Center for Advanced Brain Imaging, Georgia State University, Atlanta, Georgia 30303-4106, USA*
(Received 28 May 2013; revised manuscript received 24 August 2013; published 19 September 2013)

Accurate localization of the epileptic seizure onset zones (SOZs) is crucial for successful surgery, which usually depends on the information obtained from intracranial electroencephalography (IEEG) recordings. The visual criteria and univariate methods of analyzing IEEG recordings have not always produced clarity on the SOZs for resection and ultimate seizure freedom for patients. Here, to contribute to improving the localization of the SOZs and to understanding the mechanism of seizure propagation over the brain, we applied spectral interdependency methods to IEEG time series recorded from patients during seizures. We found that the high-frequency (>80 Hz) Granger causality (GC) occurs before the onset of any visible ictal activity and causal relationships involve the recording electrodes where clinically identifiable seizures later develop. These results suggest that high-frequency oscillatory network activities precede and underlie epileptic seizures, and that GC spectral measures derived from IEEG can assist in precise delineation of seizure onset times and SOZs.

DOI: 10.1103/PhysRevE.88.030701 PACS number(s): 87.19.xm, 02.70.Hm, 02.50.Sk, 87.19.lj

Introduction. Of 2.5 million people with epilepsy in the United States, at least 30% have seizures such as refractory temporal lobe epilepsy that cannot be controlled with medication, and are therefore potential candidates for epilepsy surgery [1]. But 10%–40% of patients who undergo presurgical evaluation have seizures that are not localized by the use of scalp electroencephalography (EEG), multimodal imaging, and magnetoencephalography (MEG). Many of these patients undergo intracranial electroencephalography (IEEG) recording with grid and depth electrodes. However, the increasing numbers of electrodes implanted by neurosurgeons in recent years often totaling over 100 per patient have not always produced greater clarity. Sampling of the seizure onset zone may still be incomplete. IEEG seizures may appear nonlocalized by conventional visual standards. Complete resection or disconnection of an apparent, nonlesional, extratemporal focus leads to a cure in less than 50% of cases. Traditional criteria for the estimation of IEEG seizure onset may be inadequate for many patients.

A conventional evaluation for epilepsy surgery uses IEEG to record a number of seizures, typically three to ten, over a period of 1–4 weeks during an inpatient stay in the epilepsy monitoring unit. From the recorded information, the epilepsy monitoring team and neurosurgeons try to estimate the seizure onset zone (SOZ) in preparation for surgery. Suggested methods for the evaluation of IEEG include extending expert analysis of conventional visual EEG frequencies to direct current (dc) shift to high beta (20–30 Hz) to gamma (30–100 Hz) frequencies, and more recently to interictal high-frequency (>80 Hz) oscillations (HFOs) [2–4]. Epilepsy surgery restricted mainly to the brain regions of HFOs has often lead to seizure freedom [2,5]. However, HFOs are also commonly observed in a normal brain state [3]. Various measures (linear and nonlinear, univariate and bivariate) have been used to discriminate a preictal state from an interictal period [6]. The univariate methods have not always been sufficient in identifying the crucial ictal portion. The bivariate methods used so far have not been able to reveal the importance of high-frequency network activity in localizing epileptic seizure onsets. Nonlinear time series techniques have been mostly applied to predict seizures from the ictal activity of brain potential recordings [7]. However, the suitability of nonlinear measures to characterize brain potential recordings in predicting seizures has been questioned [8].

The activity of pathological neuronal systems and their network interactions lie at the heart of epileptic seizure and its propagation over the brain [9]. Current IEEG monitoring practice is still in the process of realizing the underlying network mechanisms of the generation and propagation of epileptic seizures. A limited number of studies have applied network correlational measures such as correlation and coherence to epilepsy data [10]. Here, considering neuronal network dynamics and HFOs at the heart of seizure generation and propagation over the brain, we applied multivariate spectral interdependency techniques to IEEG recordings of eight patients, including the directional measure Granger causality (GC), and assessed their effectiveness in the localization of seizure onset times and zones.

Fourier and wavelet transform-based nonparametric methods were recently extended to obtain Granger causality spectra [11,12]. Granger causality spectra can be used to examine the strengths, directions, and frequencies of interactions between oscillatory stochastic processes. Clive J. Granger, 2003's Nobel Laureate in Economics, had formulated the statistical definition of time-domain causality between two jointly stationary processes in 1969 using a parametric modeling scheme of time series data [13]. The frequency-domain Granger causality under the same parametric estimation approach was proposed by Geweke in 1982 [14]. The parametric and nonparametric approaches to spectral analysis of time series data are complementary to each other [11]. In this Rapid Communication, we used both parametric and nonparametric approaches for optimal estimation of spectral quantities such as power, coherence, and Granger causality from spatially

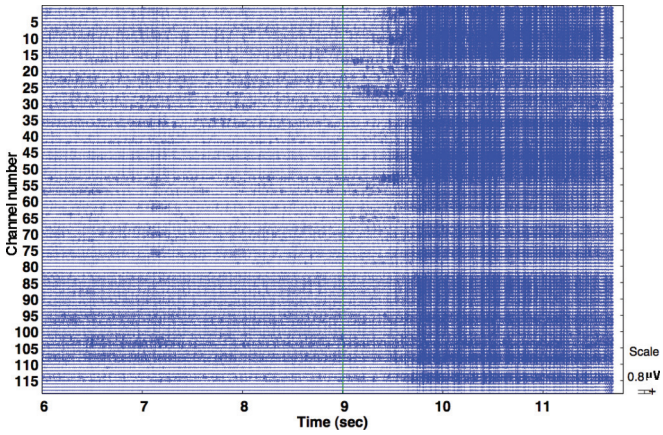

FIG. 1. (Color online) Sample time series: Multichannel IEEG recordings with a seizure event in a patient. A green vertical line at $t = 9.0$ s marks the beginning time of a visually identified seizure event.

distributed IEEG recordings. We also computed total interdependence (TI) by integrating coherence over the entire frequency range [14] and net causal outflow (OF) associated with each recording electrode. With these measures, we evaluated where and when seizures started and how they propagated over the recording electrodes implanted in the subdural space and directly within the brain.

Materials and methods: *Spectral interdependency measures*. Here, we first define spectral measures from two simultaneously measured time series, $\mathbf{x}$: $x_1(1), x_1(2), \ldots, x_1(t), \ldots$ and $\mathbf{y}$: $y(1), y(2), \ldots, y(t), \ldots$, where the sampling rate of measurement is f_s. Using either a parametric or a nonparametric spectral estimation approach [11,12], we can obtain the spectral density matrix $[\mathbf{S}(f)]$, transfer function $[\mathbf{H}(f)]$, and noise covariance matrix (Σ) from these time series. For nonstationary processes, the wavelet transform-based nonparametric estimation [11] can be used and these quantities become functions of both time and frequency indices. Time-domain total interdependence (TI) between these two processes is a measure to reflect the total amount of mutual information and is defined in terms of coherence $C(f)$ between them [14]:

$$TI_{x,y} = -\frac{1}{f_s}\int_0^{f_s} \ln\left[1 - C(f)\right] df. \tag{1}$$

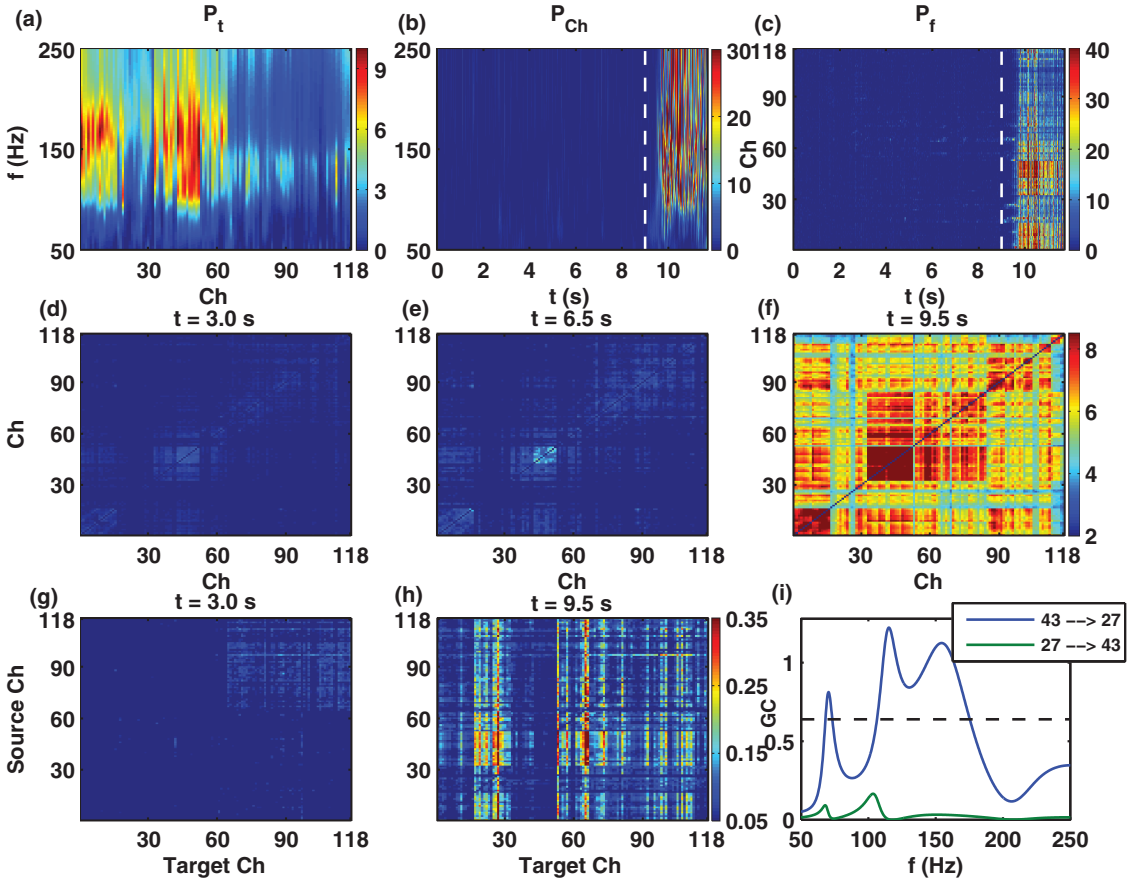

FIG. 2. (Color online) Spectral power averages, total interdependence (TI), and time-domain Granger causality (GC). (a)–(c) Wavelet power (z score) averaged over time (a), over recording channel (b), and over frequency (c). The white dashed lines in (b) and (c) represent the seizure onset times assessed by using traditional visual criteria. (d)–(f) TI at different times ($t = 3.0$, 6.5, and 9.5 s). In the ictal period ($t = 9.5$ s) the seizure has already spread to the entire network (f). (g)–(h) Time-domain GC in preictal period ($t = 3.0$ s) and the ictal period ($t = 9.5$ s). (i) Frequency-domain Granger causality spectra for two selected channels, 43 and 27, in which the former sends a dominantly stronger causal influence to the latter at around $t = 9.5$ s. The horizontal dashed line represents the threshold level at significance $p < 10^{-6}$, obtained by permutation tests.

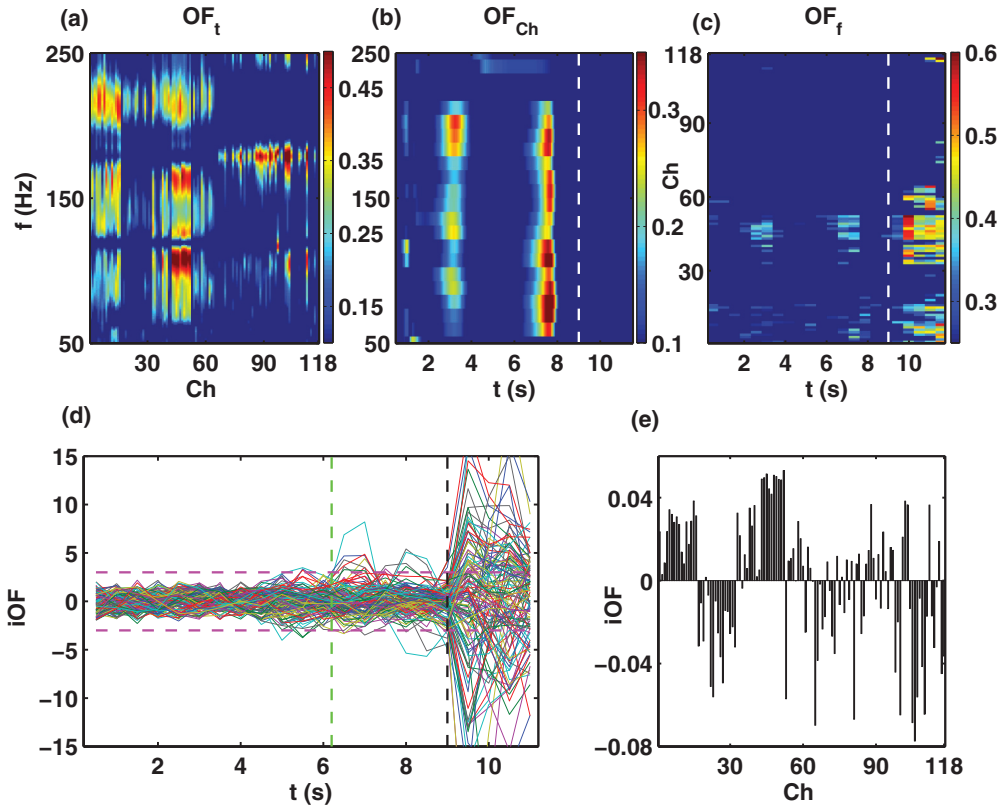

FIG. 3. (Color online) The net causal outflow (OF) averaged over time (a), over recording channel (b), and over frequency (c). The white dashed lines [(b) and (c)] represent the seizure onset times assessed by the traditional visual criteria. (d) Integrated net causal outflows (iOF, expressed in z score). iOF crosses three standard deviations (marked by horizontal dashed lines) ~3 s earlier (marked by a vertical green line at around 6 sec) than the time assessed by using the traditional criteria (marked by a dashed black line). (e) iOF after the time of significant causality from all IEEG recordings of the same representative patient. Here, a channel with a positive value represents a causality source channel whereas one with a negative value represents a sink channel.

The coherence function $C(f)$ is defined as

$$C(f) = \frac{|S_{xy}(f)|^2}{S_{xx}(f)S_{yy}(f)}, \tag{2}$$

where $S(f)$ is the spectral matrix that contains cross spectra (S_{xy}, S_{yx}) and autospectra (power) (S_{xx}, S_{yy}). Granger causality from $\mathbf{y}$ to $\mathbf{x}$ in the spectral domain $[I_{y\to x}(f)]$ can be obtained as

$$I_{y\to x}(f) = -\ln \frac{S_{xx}(f) - \left(\Sigma_{yy} - \frac{\Sigma_{xy}^2}{\Sigma_{xx}}\right)|H_{xy}(f)|^2}{S_{xx}(f)}, \tag{3}$$

where, by interchanging x and y, one can also compute Granger causality from the first node $\mathbf{x}$ to the second node $\mathbf{y}$ at frequency f: $I_{x\to y}(f)$. The time-domain Granger causality $(F_{y\to x})$ is obtained by integration over the entire frequency range:

$$F_{y\to x} = \frac{1}{f_s}\int_0^{f_s} I_{y\to x}(f)df. \tag{4}$$

Geweke showed that $TI_{x,y} = F_{x\to y} + F_{y\to x} + F_{x.y}$ [14], where $F_{x.y}$ is instantaneous causality between $\mathbf{x}$ and $\mathbf{y}$ unlike $F_{x\to y}$ and $F_{y\to x}$, which are causalities for delayed interactions.

These measures can be computed for a number of recording channels in pairwise combinations in a moving time window (t_w). In the case of N recordings, the net causal outflow spectra $[OF(t_w, f)]$ from a node m defines the driving strength from that node around time t_w:

$$OF_m(t_w, f) = \frac{1}{N-1}\sum_{i=1}^{N}[I_{m\to i}(t_w, f) - I_{i\to m}(t_w, f)], \tag{5}$$

where the self-causality $I_{m\to i} = 0$ for all $i = m$. The integrated outflow (iOF) over frequency gives the time-domain outflow. Here, a positive OF refers to the net outgoing information flow away from the node (source) and a negative OF refers to the net incoming flow towards the node (sink). This interpretation is valid within the same patient's data. However, very low temporal resolution of the recordings may lead to spurious causalities, as was indicated in previous studies [15]. In this study, we computed wavelet power, TI, GC spectra, and OF spectra in moving time windows of each length 0.5 s (250 time points). Here from IEEG recordings, power provides us the information about the level of synchrony of the underlying neural system within a recording site, coherence about synchrony between the neuronal systems, and GC about the directed influence from one neuronal system to another.

Patient selection. IEEGs were analyzed from eight patients who had undergone electrode implantation between 2010 and 2012, using combinations of standard depth electrodes and subdural grids, recording from a total of 40–128 electrodes at

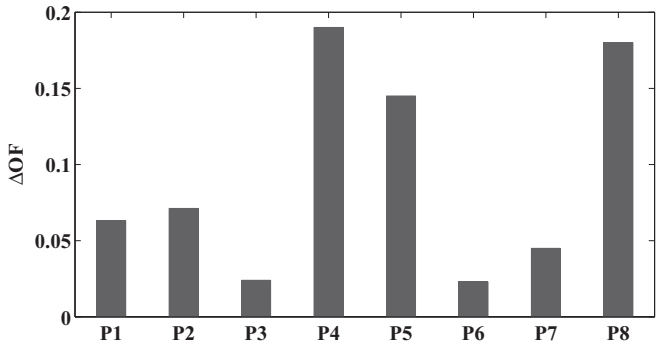

FIG. 4. Integrated causal outflow differences (ΔOF) in a source channel between ictal and preictal periods in eight patients (P1–P8). Positive differences in all patients suggest that the causality can always increase in going from the preictal to the ictal periods.

a sampling rate of 500 Hz. Raw data was saved at a passband from dc to 500 Hz. Prior to digitization, analog data was passed through a type II Chebyshev filter with a 3 db point at 240 Hz. Patients were studied retrospectively, in order to examine the general features of spectral measures in IEEG. These records were chosen because seizures appeared to have a consistent pattern of propagation, in which the onset was nonetheless ambiguous in terms of visual criteria including classic EEG frequencies, dc shifts, and gamma activity. EEG segments for analysis ranged from 5 to 20 s in duration, chosen to precede to the earliest visual manifestation of the seizure, and extending to include its visible propagation to at least two electrodes. Additional samples were taken at earlier times if high-frequency GC could be detected at the onset of the initial data segment, and separate samples were taken at times remote from known seizures, to evaluate the possible presence of GC interictally. The spectral power, coherence, and GC analyses were done on deidentified data without any specific assumptions about the seizure onset zones established by the clinical visual criteria. This study was approved by the Emory University Institutional Review Board.

Results. IEEG segments were selected from patients undergoing clinical evaluation for epilepsy surgery. These segments included clinically identified ictal (seizure) activities and interictal (away from seizure) activity. Figure 1 shows a sample of multichannel IEEG time series that includes a seizure event. In this case, the seizure was clinically determined to start at around 9 s, as marked by the green vertical line in Fig. 1. We computed wavelet power, coherence, TI, spectral and temporal GC, and net causal outflow OF as defined above from all patients separately. For this representative patient, these quantities are shown in Figs. 2 and 3. The wavelet power [Figs. 2(a)–2(c)] shows that there was high-frequency ($\sim$150 Hz) activity in a limited group of electrodes early during the seizure. Compared to $t = 3.0$ s (preictal period) in Fig. 2(d) and $t = 6.5$ s ($\sim$seizure onset time from the GC approach) in Fig. 2(e), the whole network was affected by the seizure propagation at 9.5 s (ictal period) as shown by TI [Fig. 2(f)]. A group of recordings (around channel 40) acted as strong sources of GC [Fig. 2(h)]. For instance, channel 43 was exerting a stronger causal influence to 27 than the other way around [Fig. 2(i)]. Figures 3(a)–3(e) show that the net causal outflow can identify the locations and time of seizure onset. Here, electrodes around channel 40 propagated high-frequency activities approximately 3 s before it was clinically recognized by using any visual criterion. The difference in the causal outflow between the times of seizure and before seizure for a strongest causality source remained positive for all patients P1–P8 (shown in Fig. 4). For individual outflow spectra from all patients and for further TI, iGC, and iOF results, please see the Supplemental Material [16]. In all patients, high-frequency GC relationships could be defined among groups of electrodes prior to the onset of any visible ictal activity. GC calculation shows the seizure occurred anywhere between 2.0 and 12.5 s (mean $\pm$ standard error of mean $= 6.3 \pm 1.4$ s) earlier than the time it was determined visually. For these seizure samples, the net causal outflow has exceeded three standard deviations (SD) and the positive predictive value of this finding prior to visible seizure onset was 100%. For the interictal data, which was comparable in length to the ictal data far away from seizures, the net causal outflow never exceeded 2.5 SD. Here, the most striking finding was the frequent demonstration of strong causality at frequencies approaching 200 Hz. The clinicians in the epilepsy monitoring unit were unable to visualize this activity using any combination of gain, time scale, and filter settings. Even on Fourier spectral graphs, it was detectable only by careful adjustment of display parameters. These results show that high-frequency GC could often be defined among groups of electrodes long before the onset of any visible ictal activity.

Conclusions. Identifying targets for epilepsy surgery remains a complex and imperfect process. Recent cases of seizure-free outcomes after resection of HFO-generating brain tissues [5,17] hint toward the important characteristics of the epileptogenic zone and are highly encouraging. Here, we provide evidence that high-frequency network activities are the precursors of epileptic seizures, and a careful evaluation of causal relationships from IEEG recordings can supplement the conventional visual inspection in identifying seizure onset zones for surgery. These findings suggest that high-frequency (>80 Hz) events in IEEG recordings that are close to seizure onset zones can be observed, and their causal relationships with the rest of the recordings can assist in surgical localization, thereby increasing cure rates in many patients.

Acknowledgments. A Brains and Behavior seed grant at Georgia State University to M.D. financially supported this work. M.D. was also financially supported by a US National Science Foundation (NSF) CAREER Award (No. BCS 0955037).

[1] J. A. French *et al.*, Neurology **62**, 1261 (2004); T. Dua, H. M. de Boer, L. L. Prilipko, and S. Saxena, Epilepsia **47**, 1225 (2006).

[2] P. N. Modur, S. Zhang, and T. W. Vitaz, Epilepsia **52**, 1792 (2011).

[3] R. J. Staba and A. Bragin, Biomarkers Med. **5**, 545 (2011).

[4] L. Andrade-Valenca, F. Mari, J. Jacobs, M. Zijlmans, A. Olivier, J. Gotman, and F. Debeau, Clin. Neurophysiol. **123**, 100 (2012).

[5] J. Y. Wu, R. Sankar, J. T. Lerner, J. H. Matsumoto, H. V. Vinters, and G. W. Mathern, Neurology **75**, 1686 (2010).

[6] F. Mormann, T. Kreuz, C. Rieke, R. G. Andrzejak, A. Kraskov, P. David, C. E. Elger, and K. Lehnertz, Clin. Neurophysiol. **116**, 569 (2005).

[7] M. Le Van Quyen, J. Martinerie, C. Adam, and F. J. Varela, Phys. Rev. E **56**, 3401 (1997); S. J. Schiff, Nat. Med. **4**, 1117 (1998); R. Quian Quiroga, J. Arnhold, K. Lehnertz, and P. Grassberger, Phys. Rev. E **62**, 8380 (2000); J. C. Sackellares, D. S. Shiau, L. D. Iasemidis, P. M. Pardalos, W. Chaovalitwongse, and P. R. Carney, Ann. Neurol. **52**, S65 (2002); R. Aschenbrenner-Scheibe, T. Maiwald, M. Winterhalder, H. U. Voss, J. Timmer, and A. Schulze-Bonhage, Brain **126**, 2616 (2003); K. Lehnertz, J. Biol. Phys. **34**, 253 (2008).

[8] Y.-C. Lai, M. A. F. Harrison, M. G. Frei, and I. Osorio, Phys. Rev. Lett. **91**, 068102 (2003); M. A. F. Harrison, I. Osorio, M. G. Frei, S. Asuri, and Y.-C. Lai, Chaos **15**, 033106 (2005).

[9] A. Bragin, C. L. Wilson, and J. Engel, Jr., Epilepsia **41**, S144 (2000).

[10] H. P. Zavari, W. J. Williams, J. C. Sackellares, A. Beydoun, R. B. Duckrow, and S. S. Spencer, Clin. Neurophysiol. **110**, 1717 (1999); C. A. Schevon, J. Cappell, R. Emerson, J. Isler, P. Grieve, R. Goodman *et al.*, NeuroImage **35**, 140 (2007); K. Elisevich, N. Shukla, J. E. Morgan, B. Smith, L. Schultz, K. Mason, G. L. Barkley, N. Tepley, V. Gumenyuk, and S. M. Bowyer, Epilepsia **52**, 1110 (2011); T. Gazit, I. Doron, O. Sagher, M. H. Kohrman, V. L. Towle, M. Teicher, and E. Ben-Jacob, J. Neurosci. Methods **194**, 358 (2011).

[11] M. Dhamala, G. Rangarajan, and M. Ding, Phys. Rev. Lett. **100**, 018701 (2008); NeuroImage **41**, 354 (2008).

[12] M. Ding, Y. Chen, and S. Bressler, in *Handbook of Time Series Analysis: Recent Theoretical Developments and Applications*, edited by B. Schelter, M. Winterhalder, and J. Timmers (Wiley-VCH, Berlin, 2006), pp. 437–459.

[13] C. W. J. Granger, Econometrica **37**, 424 (1969).

[14] J. Geweke, J. Am. Stat. Assoc. **77**, 304 (1982).

[15] C. A. Sims, Econometrica **39**, 545 (1971); D. A. Smirnov and B. P. Bezruchko, Europhys. Lett. **100**, 10005 (2012); D. A. Smirnov, Phys. Rev. E **87**, 042917 (2013).

[16] See Supplemental Material at http://link.aps.org/supplemental/10.1103/PhysRevE.88.030701 for individual results of all patients.

[17] J. Jacobs, M. Zijlmans, R. Zelmann, C.-E. Chatillon, J. Hall, A. Olivier, F. Dubeau, and J. Gotman, Ann. Neurol. **67**, 209 (2010).